New approximate method for calculating three-dimensional magnetic fields in laminated cores

Takayoshi Nakata
Okayama University

N. Takahashi
Okayama University

Y. Kawase
Okayama University

NEW APPROXIMATE METHOD FOR CALCULATING THREE-DIMENSIONAL MAGNETIC FIELDS IN LAMINATED CORES

T.Nakata, N.Takahashi and Y.Kawase

ABSTRACT

A new approximate method for calculating three-dimensional magnetic fields in laminated cores has been developed by modifying the two-dimensional finite element method. Using this new method, both computer storage and computing time can be considerably reduced compared with a three-dimensional analysis.

In this paper, the new technique is explained, and then its usefulness is shown by applying it to the analysis of flux distributions at the T-joint of the so-called scrap-less type three-phase transformer core.

1. INTRODUCTION

At the T-joint of the so-called scrap-less type three-phase transformer core made of grain-oriented silicon steel, the laminations are alternately turned over so that the angle between the rolling directions of overlapping sheets is 90°[1]. In such laminations, the flux distribution in one layer is different from that in the adjacent one. Thus a three-dimensional analysis is required. If an approximate analysis of such three-dimensional fields is possible by modifying the two-dimensional finite element method, both computer storage and computing time can be considerably reduced.

A new approximate method for calculating three-dimensional magnetic fields in laminated cores has been developed by introducing the "flux distribution ratio [2]" defined in 2.2. An economical analysis of the flux distribution in each layer has become possible using the new method.

2. ANALYSIS

2.1 Analyzed Model

Figure 1 shows the so-called scrap-less type three-phase transformer core. Laminations are alternately turned over. The solid arrows ⟷ denote the rolling directions of the grain-oriented silicon steel sheets in the first layer and the dashed arrows ←--→ denote those in the adjacent layer. In the hatched parts of Fig.1, the angle between the rolling directions of the adjacent sheets is 90°.

2.2 Flux Density in Each Sheet

Figure 2 shows the cross-section of the core along the line α-α' in Fig.1. As the laminations are alternately turned over, it is sufficient to discuss the behaviour of fluxes in only the two layers in Fig.2. The magnetic reluctance in the x-direction of the first layer is different from that of the second layer. Therefore, the flux Φ_{X1} in the first layer is different from the flux Φ_{X2} in the second layer.

The x-components B_{X1} and B_{X2} of the flux densities in the first and second layers shown in Fig.2 are denoted by

$$B_{X1}=\Phi_{X1}/t=\Phi_X F_{X1}/t\ , \quad (1)$$

$$B_{X2}=\Phi_{X2}/t=\Phi_X F_{X2}/t\ , \quad (2)$$

The authors are with the Department of Electrical Engineering, Okayama University, Okayama 700, Japan.

where Φ_X, Φ_{X1} and Φ_{X2} are the x-components of the total flux in the two layers, the flux in the first layer and the flux in the second layer, respectively. These are the fluxes per 1(m) in the y-direction. "t" is the effective thickness of one sheet in the z-direction. The flux distribution ratios F_{X1} and F_{X2} in each element are defined as follows:

$$F_{X1}=\Phi_{X1}/\Phi_X\ , \quad (3)$$

$$F_{X2}=\Phi_{X2}/\Phi_X=1-F_{X1}\ . \quad (4)$$

The total flux Φ_X can be written, in terms of the vector potential A, as follows [3]:

$$\Phi_X=2t\partial A/\partial y\ . \quad (5)$$

By substituting Eqs.(4) and (5) into Eqs.(1) and (2), the flux densities B_{X1} and B_{X2} can be rewritten in terms of A and F_{X1} as follows:

$$B_{X1}=2F_{X1}\,\partial A/\partial y\ , \quad (6)$$

$$B_{X2}=2(1-F_{X1})\partial A/\partial y\ . \quad (7)$$

The y-components B_{Y1} and B_{Y2} of the flux densities in the first and second layers can also be derived in the same way and written as follows:

$$B_{Y1}=-2F_{Y1}\,\partial A/\partial x\ , \quad (8)$$

$$B_{Y2}=-2(1-F_{Y1})\partial A/\partial x\ , \quad (9)$$

where the flux distribution ratio F_{Y1} is defined by

$$F_{Y1}=\Phi_{Y1}/\Phi_Y\ . \quad (10)$$

Φ_{Y1} and Φ_Y are the y-components of the flux in the first layer and of the total flux respectively.

2.3 Calculation of Energy, Vector Potentials and Flux Distribution Ratios

In our new approximate method, the vector potentials {A} and the flux distribution ratios $\{F_{X1}\}$ and $\{F_{Y1}\}$ are calculated under the minimum energy principle. The total energy X of the two layers in Fig.2 can be expressed as

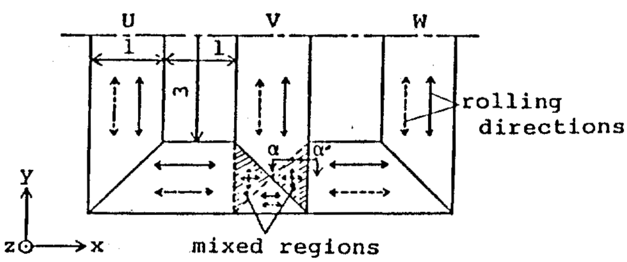

Fig.1 Three-phase transformer core.

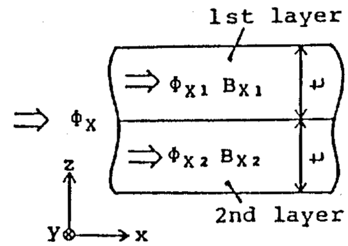

Fig.2 Section α-α' of laminated core.

0018-9464/85/1100-2374$01.00©1985 IEEE

$$X=X_1+X_2\ , \tag{11}$$

where X_1 and X_2 are the energies in the first and second layers, and these are given by

$$X_1=X_{x1}+X_{y1}\ , \tag{12}$$

$$X_2=X_{x2}+X_{y2}\ , \tag{13}$$

$$X_{x1}=t\iint_s\left(\int_0^{B_{x1}}\nu_{x1}B_{x1}dB_{x1}\right)dxdy, \tag{14}$$

$$X_{y1}=t\iint_s\left(\int_0^{B_{y1}}\nu_{y1}B_{y1}dB_{y1}\right)dxdy, \tag{15}$$

$$X_{x2}=t\iint_s\left(\int_0^{B_{x2}}\nu_{x2}B_{x2}dB_{x2}\right)dxdy, \tag{16}$$

$$X_{y2}=t\iint_s\left(\int_0^{B_{y2}}\nu_{y2}B_{y2}dB_{y2}\right)dxdy. \tag{17}$$

In Eqs.(14)-(17), it is assumed that the z-components of the fluxes and eddy currents are neglected, and the energy in each layer can be calculated using the x- and y-components of reluctivities. S denotes the region to be analyzed, and ν_{x1}, ν_{x2}, ν_{y1} and ν_{y2} are the x- and y-components of the reluctivities in the first and second layers, respectively.

In a laminated core, as the z-component of the flux density is very small compared with the x- or y-component, the above-mentioned assumption is acceptable, when the interlaminar air gap between the sheets is very small compared with the thickness of the sheet.

In order to calculate both the flux distributions in the first and second layers, not only the vector potentials $\{A\}$ but also the flux distribution ratios $\{F_{x1}\}$ and $\{F_{y1}\}$ are treated as independent variables. The following equations are obtained under the minimum energy principle:

$$\frac{\partial X}{\partial A_i}=0 \quad (i=1,---,n)\ , \tag{18}$$

$$\frac{\partial X}{\partial F_{x1}^{(e)}}=0 \quad (e=1,---,ne)\ , \tag{19}$$

$$\frac{\partial X}{\partial F_{y1}^{(e)}}=0 \quad (e=1,---,ne)\ , \tag{20}$$

where Ai is the vector potential at node i. The suffix (e) denotes the element e. n is the number of nodes at which the vector potential is unknown, and ne is the number of elements in the region to be analyzed.

Although, only the case of two kinds of layers with different magnetic reluctances is discussed here, the analysis of the case of m kinds of layers is possible by introducing 2(m-1) kinds of distribution factors.

2.4 Finite Element Formulation

The energy X is a nonlinear function of the vector potentials $\{A\}$ and the flux distribution ratios $\{F_{x1}\}$ and $\{F_{y1}\}$. Therefore, it is difficult to solve Eqs.(18), (19) and (20) directly and so an iterative technique is introduced.

(a) Discretization of Eq.(18)

The derivative of X in Eq.(18) with respect to the vector potential Ai is given as follows from Eqs.(11)-(13):

$$\frac{\partial X}{\partial A_i}=\frac{\partial}{\partial A_i}(X_{x1}+X_{y1}+X_{x2}+X_{y2})\ . \tag{21}$$

From Eq.(14), $\partial X_{x1}/\partial A_i$ is given by

$$\frac{\partial X_{x1}}{\partial A_i}=\frac{\partial X_{x1}}{\partial B_{x1}}\frac{\partial B_{x1}}{\partial A_i}$$

$$=t\iint_s\frac{\partial B_{x1}}{\partial A_i}\nu_{x1}B_{x1}dxdy, \tag{22}$$

where, $\{F_{x1}\}$ and $\{F_{y1}\}$ are assumed to be known.

Any kinds of elements, such as high-order element, isoparametric element etc., can be used for the discretization of Eq.(22). For simplicity, a first-order triangular element is used here. B_{x1} can be written as follows from Eq.(6):

$$B_{x1}=2F_{x1}\sum_{k=1}^{3}\frac{\partial N_k}{\partial y}A_k\ , \tag{23}$$

Where, N_k is an interpolation function [3] of a first-order triangular element associated with node k. From Eqs.(22) and (23), $\partial X_{x1}/\partial A_i$ can be rewritten as

$$\frac{\partial X_{x1}}{\partial A_i}=4tF_{x1}^2\iint_s\nu_{x1}\frac{\partial N_i}{\partial y}\sum_{k=1}^{3}\frac{\partial N_k}{\partial y}A_k dxdy. \tag{24}$$

The derivative of X_{y1}, X_{x2} and X_{y2} with respect to Ai can be calculated in the same way, and the final $\partial X/\partial A_i$ is given by

$$\frac{\partial X}{\partial A_i}=t\iint_s\sum_{k=1}^{3}\left\{4(F_{x1}^2\nu_{x1}+F_{x2}^2\nu_{x2})\frac{\partial N_i}{\partial y}\frac{\partial N_k}{\partial y}+4(F_{y1}^2\nu_{y1}+F_{y2}^2\nu_{y2})\frac{\partial N_i}{\partial x}\frac{\partial N_k}{\partial x}\right\}A_k dxdy. \tag{25}$$

In the nonlinear analysis using the Newton-Raphson iteration technique [3], the increments $\{\delta A_j\}$ are obtained from the following equation:

$$\left[\frac{\partial^2 X}{\partial A_i\partial A_j}\right]\left\{\delta A_j\right\}=-\left\{\frac{\partial X}{\partial A_i}\right\}. \tag{26}$$

$\partial^2 X/\partial A_i\partial A_j$ is given as follows from Eqs.(11)-(13):

$$\frac{\partial^2 X}{\partial A_i\partial A_j}=\frac{\partial^2}{\partial A_i\partial A_j}(X_{x1}+X_{y1}+X_{x2}+X_{y2})\ . \tag{27}$$

$\partial^2 X_{x1}/\partial A_i\partial A_j$ is obtained from Eq.(24) as follows:

$$\frac{\partial^2 X_{x1}}{\partial A_i\partial A_j}=4tF_{x1}^2\iint_s\left(\nu_{x1}\frac{\partial N_i}{\partial y}\frac{\partial N_j}{\partial y}+\frac{\partial\nu_{x1}}{\partial B_{x1}^2}\frac{\partial B_{x1}^2}{\partial A_j}\frac{\partial N_i}{\partial y}\sum_{k=1}^{3}\frac{\partial N_k}{\partial y}A_k\right)dxdy. \tag{28}$$

$\partial B_{x1}^2/\partial A_j$ can be calculated as follows from Eq.(23):

$$\frac{\partial B_{x1}^2}{\partial A_j}=8F_{x1}^2\frac{\partial N_j}{\partial y}\sum_{\ell=1}^{3}\frac{\partial N_\ell}{\partial y}A_\ell\ . \tag{29}$$

From Eqs.(28) and (29), $\partial^2 X_{x1}/\partial A_i\partial A_j$ is given by

$$\frac{\partial^2 X_{x1}}{\partial A_i\partial A_j}=4tF_{x1}^2\iint_s\left(\nu_{x1}\frac{\partial N_i}{\partial y}\frac{\partial N_j}{\partial y}+8F_{x1}^2\frac{\partial\nu_{x1}}{\partial B_{x1}^2}\times\frac{\partial N_i}{\partial y}\frac{\partial N_j}{\partial y}\sum_{k=1}^{3}\frac{\partial N_k}{\partial y}A_k\cdot\sum_{\ell=1}^{3}\frac{\partial N_\ell}{\partial y}A_\ell\right)dxdy, \tag{30}$$

The derivative of X_{y1}, X_{x2} and X_{y2} with respect to Ai and Aj can be calculated in the same way, and the final $\partial^2 X/\partial A_i\partial A_j$ is given by

$$\frac{\partial^2 X}{\partial A_i\partial A_j}=t\iint_s\Big\{4(F_{x1}^2\nu_{x1}+F_{x2}^2\nu_{x2})\frac{\partial N_i}{\partial y}\frac{\partial N_j}{\partial y}+4(F_{y1}^2\nu_{y1}+F_{y2}^2\nu_{y2})\frac{\partial N_i}{\partial x}\frac{\partial N_j}{\partial x}+32\left(F_{x1}^4\frac{\partial\nu_{x1}}{\partial B_{x1}^2}+F_{x2}^4\frac{\partial\nu_{x2}}{\partial B_{x2}^2}\right)\times\frac{\partial N_i}{\partial y}\frac{\partial N_j}{\partial y}\sum_{k=1}^{3}\frac{\partial N_k}{\partial y}A_k\cdot\sum_{\ell=1}^{3}\frac{\partial N_\ell}{\partial y}A_\ell+32\left(F_{y1}^4\frac{\partial\nu_{y1}}{\partial B_{y1}^2}+F_{y2}^4\frac{\partial\nu_{y2}}{\partial B_{y2}^2}\right)\frac{\partial N_i}{\partial x}\frac{\partial N_j}{\partial x}$$

$$\times \sum_{k=1}^{3} \frac{\partial N_k}{\partial x} \cdot A_k \sum_{\ell=1}^{3} \frac{\partial N_\ell}{\partial x} A_\ell \Big\} dxdy. \qquad (31)$$

(b) Discretization of Eqs.(19) and (20)

$\partial \chi / \partial F_{x1}$ and $\partial \chi / \partial F_{y1}$ are obtained from Eqs.(6)-(9) and (11)-(17) under the assumption that the vector potentials $\{A\}$ are known as follows:

$$\frac{\partial \chi}{\partial F_{x1}} = t \iint_s \left\{ \nu_{x1} F_{x1} \left(2\frac{\partial A}{\partial y}\right)^2 - \nu_{x2}(1-F_{x1})\left(2\frac{\partial A}{\partial y}\right)^2 \right\} dxdy = 0, \qquad (32)$$

$$\frac{\partial \chi}{\partial F_{y1}} = t \iint_s \left\{ \nu_{y1} F_{y1} \left(-2\frac{\partial A}{\partial x}\right)^2 - \nu_{y2}(1-F_{y1})\left(-2\frac{\partial A}{\partial x}\right)^2 \right\} dxdy = 0. \qquad (33)$$

ν_{x1}, ν_{x2}, ν_{y1} and ν_{y2} are functions of B_{x1}, B_{x2}, B_{y1} and B_{y2}. The flux densities are the functions of F_{x1} and F_{y1}. Therefore, Eqs.(32) and (33) are nonlinear equations of F_{x1} and F_{y1}. F_{x1} and F_{y1} can be calculated by the Newton iteration technique. The increments δF_{x1} and δF_{y1} are given by

$$\frac{\partial^2 \chi}{\partial F_{x1}^2} \delta F_{x1} = -\frac{\partial \chi}{\partial F_{x1}}, \qquad (34)$$

$$\frac{\partial^2 \chi}{\partial F_{y1}^2} \delta F_{y1} = -\frac{\partial \chi}{\partial F_{y1}}. \qquad (35)$$

$\partial^2 \chi / \partial F_{x1}^2$ and $\partial^2 \chi / \partial F_{x2}^2$ are given by

$$\frac{\partial^2 \chi}{\partial F_{x1}^2} = t \iint_s \left(2\frac{\partial A}{\partial y}\right)^2 \left\{ \nu_{x1} + \nu_{x2} + 2\left(2\frac{\partial A}{\partial y}\right)^2 \left\{ F_{x1}^2 \frac{\partial \nu_{x1}}{\partial B_{x1}^2} + (1-F_{x1})^2 \frac{\partial \nu_{x2}}{\partial B_{x2}^2} \right\} \right\} dxdy, \qquad (36)$$

$$\frac{\partial^2 \chi}{\partial F_{y1}^2} = t \iint_s \left(-2\frac{\partial A}{\partial x}\right)^2 \left\{ \nu_{y1} + \nu_{y2} + 2\left(-2\frac{\partial A}{\partial x}\right)^2 \left\{ F_{y1}^2 \frac{\partial \nu_{y1}}{\partial B_{y1}^2} + (1-F_{y1})^2 \frac{\partial \nu_{y2}}{\partial B_{y2}^2} \right\} \right\} dxdy. \qquad (37)$$

2.5 Calculation

Figure 3 shows the steps of calculation.

①: The initial values of vector potentials $\{A\}$ and flux distribution ratios $\{F_{x1}\}$ and $\{F_{y1}\}$ are set.
②: The increments of the vector potentials $\{\delta A\}$ can be calculated from Eq.(26).
③: The increments of flux distribution ratios $\{\delta F_{x1}\}$ and $\{\delta F_{y1}\}$ are calculated from Eqs.(34) and (35). $\{\varepsilon_1\}$ and $\{\varepsilon_2\}$ are small numbers for the decision of convergence.
④: The above steps are repeated alternately until the final solution is obtained. $\{\varepsilon_0\}$ is a small number for determining convergence.

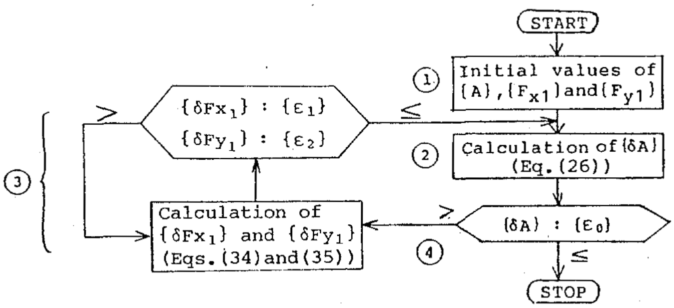

Fig.3 Flow chart.

3. APPLICATION

The flux distribution in each layer of the T-joint of a three-phase transformer core denoted in Fig.1 has been calculated. The core is made of 0.35 (mm) thick grain-oriented silicon steel M-5. The dimensions of the core are shown in Fig.1.

Figure 4 shows the flux density vectors in each layer of the T-joint. The overall flux density Bleg in the limb is 1.7(T). The arrows denote the amplitude and the direction of the flux density vector in each element. The directions of fluxes near the corner of the window in the T-joint are almost the same as the rolling direction. The average flux distributions of both layers in Figs. 4(a) and (b) are shown in Fig.5.

The spatial variations of the loci of the rotating flux density vectors corresponding to Fig.4(a) and Fig.5 are shown in Figs.6 and 7, respectively. The spatial distribution of the maximum flux density corresponding to Fig.4(a) is shown in Fig.8. In Fig.4(b), as the flux passing through the line a-a' wants to flow toward the corner a, the maximum flux density at the corner is beyond 2.0(T).

Figures 4 to 8 show that the apparent flux is quite different from that in each layer. Therefore, there would be a large error in estimating the iron losses from the fluxes in Figs. 5 and 7, since the iron losses

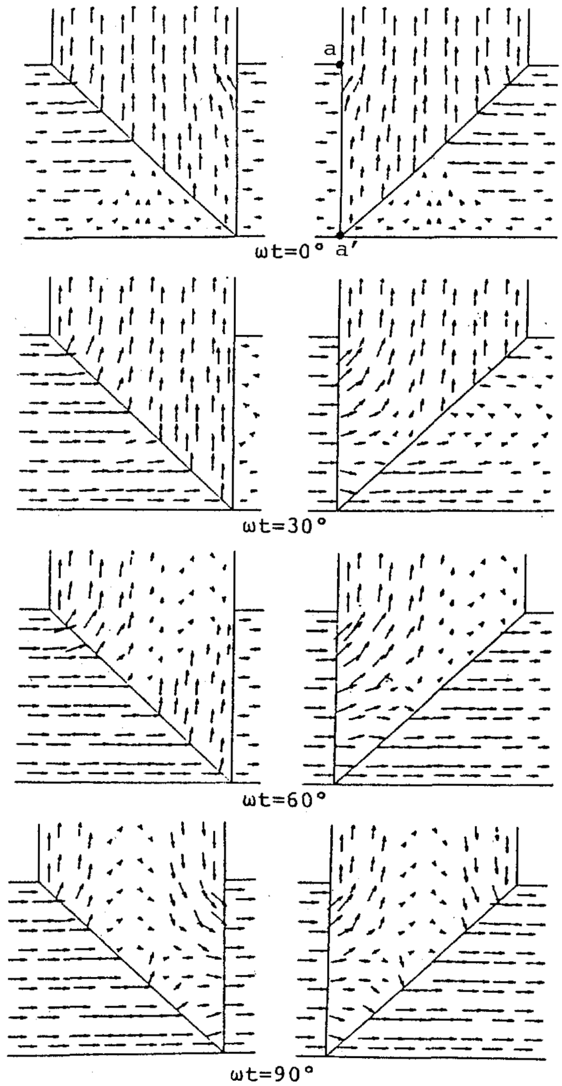

(a) first layer (b) second layer

Fig.4 Flux density vectors in each layer (M-5, 0.35mm, Bleg=1.7T).

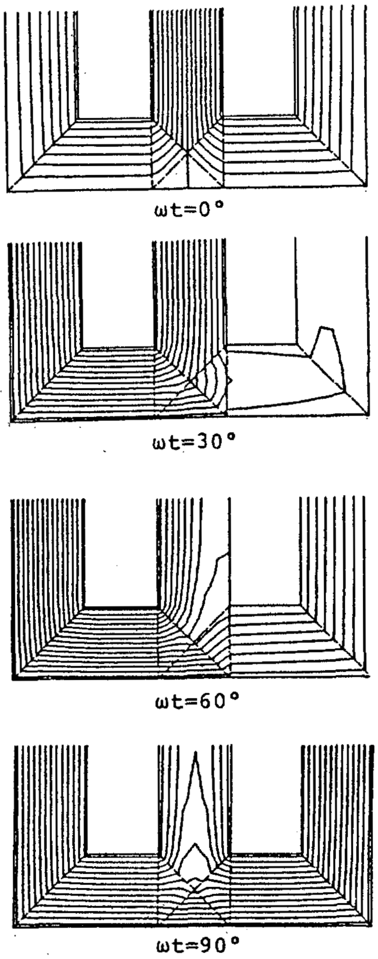

Fig.5 Apparent flux distributions (M-5, 0.35mm, Bleg=1.7T).

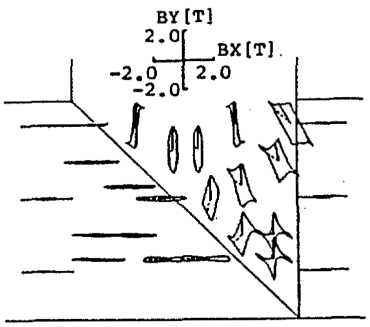

Fig.6 Loci of the flux density vectors in the first layer (M-5, 0.35mm, Bleg=1.7T).

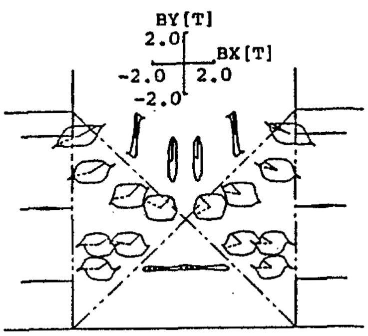

Fig.7 Loci of the apparent flux density vectors (M-5, 0.35mm, Bleg=1.7T).

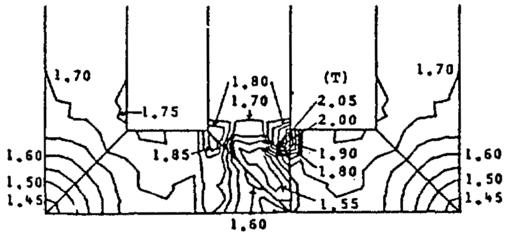

Fig.8 Distribution of the maximum flux density in the first layer (M-5, 0.35mm, Bleg=1.7T).

are a function of the fluxes in each layer denoted in Figs. 4, 6 and 8.

The results presented here were calculated within about 70(%) increase of computing time than a two-dimensional analysis.

4. CONCLUSIONS

By modifying the two-dimensional finite element method, it has become possible to analyze easily the flux distribution in each layer of laminated cores made of grain-oriented silicon steel. In our new method, the distribution of flux in each layer is determined by the minimum energy principle. The method has the following advantages:

(a) The approximate three-dimensional analysis is possible by adding several lines to the usual two-dimensional program.

(b) The computing time is within twice as much as two-dimensional one.

The results obtained provide information for designing the most suitable laminated core.

The method will be improved so that the energy due to the z-component of the flux and eddy currents can be taken into account.

ACKNOWLEDGEMENT

The authors wish to thank Mr. M. Kawata for his help in computing problems.

REFERENCES

[1] T. Nakata, N. Takahashi, Y. Kawase and M. Nakano: "Influence of Lamination Orientation and Stacking on Magnetic Characteristics of Grain-Oriented Silicon Steel Laminations", IEEE Transactions on Magnetics, Vol.MAG-20, No.5, September 1984.

[2] T. Nakata, Y. Kawase and M. Kawata: "Approximate Solution of Three-Dimensional Magnetic Field at Joints of Transformer Cores", Papers of Combined Technical Meeting on Rotating Machines and Static Apparatus, RM-83-92, SA-83-42, IEE, Japan, 1983.

[3] T. Nakata and N. Takahashi: "Finite Element Method in Electrical Engineering" (book, in Japanese), Morikita Shuppan, Tokyo, 1982.